teristics of the system and this becomes a natural extension of the method used herein.

## References


[1] Bolotin, V. V., *The Dynamic Stability of Elastic Systems*, Holden Day, 1964.

[2] Eringen, A. C., "Response of Beams and Plates to Random Loads," *Transactions of the ASME, Ser. E: Journal of Applied Mechanics*, March 1957, pp. 46–52.

[3] Hurty, W. C. and Rubenstein, M. F., *Dynamics of Structures*, Prentice Hall, Englewood Cliffs, N. J., 1965.

[4] Thompson, W. T. and Barton, M. V., "The Response of Mechanical Systems to Random Excitation," *Transactions of the ASME, Ser. E: Journal of Applied Mechanics*, June 1957, pp. 248–251.

[5] Lepore, J. A. and Shah, H. C., "Dynamic Stability of Axially Loaded Columns Subjected to Stochastic Excitations," *AIAA Journal*, Vol. 6, No. 8, Aug. 1968, pp. 1515–1521.

[6] Bertram, J. E. and Sarachik, P. E., "Stability of Circuits with Randomly Time Varying Parameters," *Proceedings of the International Symposium on Circuit and Information Theory*, Institute of Radio Engineers, New York, CT-6, 1959, pp. 260–270.

[7] Lanczos, C., *Variational Principles of Mechanics*, Univ. of Toronto, Press, Canada, 1949.

[8] Timoshenki, S. and Woinowsky, K., *Theory of Plates and Shells*, McGraw-Hill, New York, 1959.

[9] Alimov, M. S., "On the Construction of Lyaminov Functions for Systems of Linear Differential Equations with Constant Coefficients" (in Russian) *Siberian Mathematical Journal*, Vol. 2, 1961, pp. 3–6.

[10] Caughey, T. K. and Gray, A. H., "On the Almost Sure Stability of Linear Dynamic Systems with Stochastic Coefficients," *Transactions of the ASME, Ser. E: Journal of Applied Mechanics*, 1965, pp. 365–372.

[11] Kozin, F., "On Almost Sure Stability of Linear Systems with Random Coefficients," *Journal of Mathematics and Physics*, Vol. 42, 1963, pp. 59–67.

[12] Ariaratnam, S. T., *Dynamic Stability of a Column Under Random Loading*, 1967, Univ. of Waterloo, Waterloo, Ontario, Canada.

[13] Infante, E. F. and Plaut, R. H., "Stability of a Column Subjected to a Time-Dependent Axial Load," *AIAA Journal*, Vol. 7, No. 4, April 1969, pp. 766–768.


MAY 1970 J. SPACECRAFT VOL. 7, NO. 5

# Dynamic Stability of Cylindrical Propellant Tanks


DANIEL D. KANA* AND WEN-HWA CHU*

*Southwest Research Institute, San Antonio, Texas*



**Dynamic instability and associated parametric resonance is a dominant form of response in a longitudinally excited cylindrical shell containing liquid. The present paper is devoted to a theoretical and experimental study of its occurrence in a cylindrical system which includes the influences of axial preload, ullage pressure, partial liquid depth, and a finite top impedance. Donnell shell theory and a modified Galerkin procedure are utilized to formulate equations which govern the stability of perturbations superimposed on an axisymmetric initial state of response. Stability boundaries are computed for a range of parameters affecting the region of principal parametric resonance and are compared with experimental results. It is found that liquid depth, top impedance, and ullage pressure have a strong influence on stability, while the effects of axial preload are relatively insignificant.**


## Nomenclature

$a$ = radius of the shell
$c_0$ = speed of sound in the liquid
$c_s$ = $E/\rho_s$, speed of stress waves in the shell
$E$ = modulus of elasticity
$g$ = standard acceleration of gravity
$H$ = $h/a$, nondimensional liquid depth
$H_s$ = $h_s/a$, nondimensional thickness of shell
$I_z$ = mass moment of inertia of top weight about $z$ axis
$l$ = length of the shell
$m$ = one-half of the number of circumferential nodes; $\cos(m\theta)$
$N_{xxd}^*, N_{\theta\theta d}^*$ = dynamic part of initial-state stress resultants [nondimensionalized by $(1 - \nu^2)/Eh_s$]
$N_{xxs}^*, N_{\theta\theta s}^*, N_{x\theta s}^*$ = static part of initial-state stress resultants [nondimensionalized by $(1 - \nu^2)/Eh_s$]
$n$ = axial wave number; $\sin n\pi x/l$
$P_r$ = nondimensional pressure loading on shell, $p_r/E$
$P_0, p_0$ = axial preload, ullage pressure
$R,\theta,X$ = cylindrical coordinates (space-fixed) nondimensionalized by $a$
$U,V,W$ = shell displacements $u,v,w$, nondimensionalized by $a$
$X_0$ = nondimensional amplitude of axial excitation ($X_0 = \hat{x}_0/a$)
$Z_0$ = top acceleration impedance (force/acceleration)
$\beta$ = density parameter $\rho_l a/\rho_s h_s$
$\nu$ = Poisions ratio
$\Phi$ = velocity potential, nondimensionalized by $\omega_0^2 a^2/\omega_r$
$\rho_l, \rho_s$ = mass densities of liquid and shell
$\tau$ = nondimensional time, $\tau = \omega_r t$
$\omega_0^2$ = liquid parameter $c_0^2/a^2$
$\omega_r, \omega$ = response and excitation frequencies
$\omega_k$ = natural frequency of $m$, $k$-th mode
$\Omega_i^2$ = designated frequency, nondimensionalized by $a^2/c_s^2$
$\bar{\Omega}_i^2, \bar{\Omega}_i^2$ = designated frequencies, nondimensionalized by $(1 - \nu^2)a^2/c_s^2$ and by $a^2/c_0^2$, respectively

### *Superscripts*

$(\hat{})$ = the amplitude of $(\ )$
$(\dot{})$ = $(d/d\tau)(\ )$, $\tau = \omega t$
$(\ )^p$ = related to initial-state response


Presented at the AIAA Structural Dynamics and Aeroelasticity Specialist Conference, New Orleans, April 16–17, 1969 (no paper number; published in bound volume of conference papers); submitted May 5, 1969; revision received October 31, 1969. The results presented in this paper were obtained during the course of research sponsored by Marshall Space Flight Center (NASA) under Contracts NAS820329 and NAS8-21282.



* Senior Research Engineers, Department of Mechanical Sciences. Members AIAA.

## Introduction

CLASSIC examples of dynamic instability and parametric resonance have been studied in detail by Bolotin.[1] Experimental investigations[2] have shown that this type of behavior is dominant amidst a complex variety of responses which can be observed in a longitudinally excited model vehicle propellant tank which is not sufficiently reinforced with stiffeners. A theoretical and further experimental investigation[3] was conducted for a longitudinally excited, liquid-filled cylindrical shell. It was found that the system initially tends to respond in a state comprised of linear axisymmetric modes. However, the resulting membrane stresses form a parametric load with respect to nonaxisymmetric perturbations superimposed on the initial state. Thus, for wide ranges of the excitation parameters, instability and subsequent parametric resonance results, and linear vibration theory is no longer adequate to predict the response of either liquid pressure or wall motion. This paper is devoted to a study of their occurrence in a cylindrical shell system which includes the influence of axial preload, ullage pressure, partial liquid depth, and a finite top impedance. Figure 1 indicates the appropriate parameters and boundary conditions for both the initial and perturbed states. The initial state represents linear forced axisymmetric motion, whose responses have already been determined, along with natural frequencies and modal functions for the system.[4] Stability of motion in the perturbed state is the subject of the present paper, although results from Ref. 4 must be utilized in part of the analysis. Note that, theoretically, the perturbed state can be either axisymmetric ($m = 0$) or nonaxisymmetric ($m > 0$); however, for a single tank system, the nonaxisymmetric form of instability is dominant.

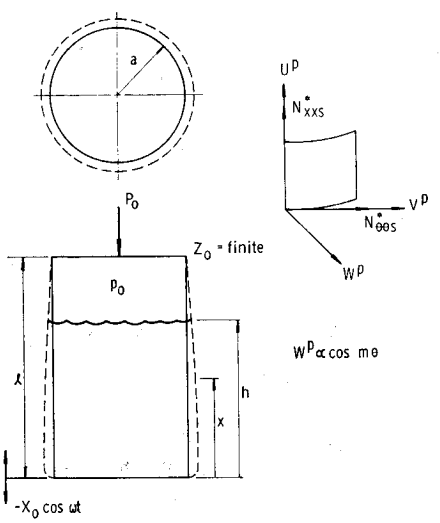


**Fig. 1a Mechanism of dynamic instability-initial state, $m = 0$.**

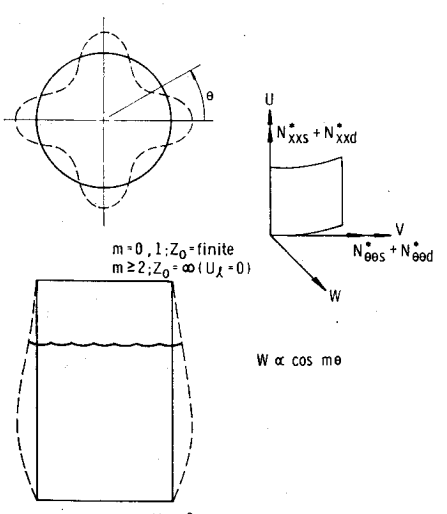


**Fig. 1b Mechanism of dynamic instability-perturbed state, $m \geq 0$.**

## Derivation of Stability Equations

The perturbed motion represented by Fig. 1b will be analyzed by means of Sander's nonlinear shell equations[5,6] which are based on Donnell approximations. These equations contain nonlinear terms resulting from the rotation of shell elements as well as nonlinear strain-displacement relations. We will follow the philosophy of Bolotin[1] and assume that retaining only nonlinear terms which result from rotations is sufficient to determine dynamic stability. Compressible flow theory is used for the liquid. The motion is expanded into a series of the natural mode eigenvectors which were obtained from the solution of the free vibration problem.[4] A modified Galerkin procedure is then utilized to reduce the system to a linear second-order, time dependent set of coupled differential equations having periodic coefficients. The method is "modified" in the sense that the natural modal functions (finite series eigenvectors) are chosen as weighting functions, although they are not of closed form. An approximation of the perturbed motion will then be obtained by the use of only one eigenvector term of the series, so that the coupled set reduces to a single stability equation.

Thus, the governing shell equations are of the form

$$F_1 = L_{11}U + L_{12}V + L_{13}W - \tilde{\Omega}_r^2 \partial^2 U/\partial\tau^2 = 0 \quad (1a)$$

$$F_2 = L_{21}U + L_{22}V + L_{23}W - \tilde{\Omega}_r^2 \partial^2 V/\partial\tau^2 = 0 \quad (1b)$$

$$F_3 = L_{31}U + L_{32}V + L_{33}W - \tilde{\Omega}_r^2 \partial^2 W/\partial\tau^2 + \epsilon_d \tilde{L}_{33} W \cos\omega t + [(1 - \nu^2)/H_s]P_r = 0 \quad (1c)$$

where

$$L_{11} = \frac{\partial^2}{\partial X^2} + \frac{1-\nu}{2}\frac{\partial^2}{\partial\theta^2}, \qquad L_{12} = \frac{1+\nu}{2}\frac{\partial^2}{\partial X \partial\theta}$$

$$L_{13} = \nu\frac{\partial}{\partial X}, \qquad L_{21} = \frac{1+\nu}{2}\frac{\partial^2}{\partial X\partial\theta} \quad (2a)$$

$$L_{22} = \frac{\partial^2}{\partial\theta^2} + \frac{1-\nu}{2}\frac{\partial^2}{\partial X^2}, \qquad L_{23} = \frac{\partial}{\partial\theta}$$

$$L_{31} = -\nu\frac{\partial}{\partial X}, \qquad L_{32} = -\frac{\partial}{\partial\theta}$$

$$L_{33} = -\left[\frac{H_s^2}{12}\left(\frac{\partial^4}{\partial X^4} + 2\frac{\partial^4}{\partial X^2\partial\theta^2} + \frac{\partial^4}{\partial\theta^4}\right) + 1\right] + \left[\frac{\partial}{\partial X}\left(N_{xxs}^*\frac{\partial}{\partial X}\right) + \frac{\partial}{\partial X}\left(N_{x\theta s}^*\frac{\partial}{\partial\theta}\right) + \frac{\partial}{\partial\theta}\left(N_{\theta x s}^*\frac{\partial}{\partial X}\right) + \frac{\partial}{\partial\theta}\left(N_{\theta\theta s}^*\frac{\partial}{\partial\theta}\right)\right] \quad (2b)$$

$$\tilde{L}_{33} = \frac{\partial}{\partial X}\left(\hat{N}_{xxd}^*\frac{\partial}{\partial X}\right) + \frac{\partial}{\partial\theta}\left(\hat{N}_{\theta\theta d}^*\frac{\partial}{\partial\theta}\right)$$

$\epsilon_d = 0$ for free vibration, $\epsilon_d = 1$ for forced vibration. Pressure loading on the shell is given by

$$[(1 - \nu^2)/H_s]P_r = -\tilde{\Omega}_0^2\beta(\partial\Phi/\partial\tau) \qquad \text{at } R = 1 \quad (3)$$

where the fluid velocity potential is governed by

$$\nabla^{*2}\Phi - \tilde{\Omega}_r^2\partial^2\Phi/\partial\tau^2 = 0 \quad (4)$$

Boundary conditions on the fluid and shell are: At $X = 0$, $U = W = V = 0$, and $\partial^2 W/\partial X^2 = 0$. At $X = l/a$, $W =$

$V = 0$, $\partial^2 W/\partial X^2 = 0$ and

$$F_4 = \partial U/\partial X + Z^{**}\tilde{\Omega}_r{}^2 \partial^2 U/\partial \tau^2 = 0 \quad (5)$$

where

$$Z^{**} = Z_0(1 - \nu^2)/(2\pi\rho_s a^2 h_s) \text{ for } m = 0$$
$$Z^{**} = (1 - \nu^2) I_z/(4\rho_s h_s a^5) \text{ for } m = 1$$
$$Z^{**} = \infty \text{ for } m \geq 2$$

Solutions of the shell motion having a given circumferential displacement distribution will be sought as expansions of the $k$-$m$th natural modes

$$U(\theta,\tau,X) = \cos m\theta \sum_{k=1}^{K} a_k(\tau) U_{mk}(X) = \sum_{k=1}^{K} a_k U_{1k} \quad (6a)$$

$$V(\theta,\tau,X) = \sin m\theta \sum_{k=1}^{K} a_k(\tau) V_{mk}(X) = \sum_{k=1}^{K} a_k U_{2k} \quad (6b)$$

$$W(\theta,\tau,X) = \cos m\theta \sum_{k=1}^{K} a_k(\tau) W_{mk}(X) = \sum_{k=1}^{K} a_k U_{3k} \quad (6c)$$

where for convenience we have defined a general shell displacement vector $\mathbf{U}(U,V,W) = \mathbf{U}(U_1,U_2,U_3)$, which is a function of both space and time and is associated with the fluid velocity potential $\Phi$ and upper shell displacement $U_l$.

The potential $\Phi$ satisfies Eq. (4) which forms a constraint on the shell system. In order to interpret the fluid pressure loading as an apparent mass which is valid at the response frequency $\omega_r$, we express the potential for forced motion as

$$\Phi(\theta,\tau,\omega_r,R,X) = \cos m\theta \sum_{k=1}^{K} \dot{a}_k(\tau) \Phi_{mk}(\omega_r,R,X) \quad (7)$$

Note that $\Phi_{mk}(\omega_r, R,X)$ is the component of $\Phi$ associated with a shell displacement component $W_{mk}$, and both liquid and shell motion is anticipated to be nearly periodic with responses at frequency $\omega_r$. At the shell wall, we use the notation $\Phi_{mk}(\omega_r,1,X) = \Phi_{mk}(\omega_r,X)$.

For the special case of $\omega_r = \omega_k$, the system responds in the $m,k$th natural mode, and the shell displacement modal functions form the vector $\mathbf{U}_k(U_{1k},U_{2k},U_{3k})$, which is a function of space only and is associated with the fluid velocity potential $\Phi_{mk}(\omega_k,X)$ and the top displacement $U_{lk}$. From the definition of natural frequencies, these modal functions satisfy

$$\sum_{j=1}^{3} L_{ij}U_{jk} + \delta_{i3}\tilde{\Omega}_0{}^2\beta\Phi_{mk}(\omega_k,X) + \tilde{\Omega}_k{}^2 U_{ik} = 0, \; i = 1,2,3 \quad (8a)$$

$$\partial U_{1k}/\partial X = Z^{**}\tilde{\Omega}_k{}^2 U_{1k} \qquad \text{at } X = l/a \quad (8b)$$

We now consider the forced motion. By means of a Galerkin procedure,[7] we form an expression for virtual work in the system

$$\sum_{i=1}^{3} \int_S F_i(\mathbf{U}) \cdot U_{ik'} dS + \epsilon_m \int_C F_4(U_{lk}) \cdot U_{lk'} d\theta = 0 \quad (9)$$

where $\epsilon_m = 1$ for $m = 0, 1$; $\epsilon_m = 0$ for $m \geq 2$. More specifically, we substitute Eqs. (3, 6 and 7) into Eqs. (1) and (5) and then by means of Eq. (9) form an expression for virtual work between forces (expressed in terms of displacements) associated with the general forced motion and displacements associated with the $m,k'$th natural mode. There results

$$\sum_{k=1}^{K}\Bigg[ a_k \int_S \sum_{i=1}^{3}\sum_{j=1}^{3} U_{ik'}(L_{ij}U_{jk}) dS -$$

$$\ddot{a}_k \int_S \tilde{\Omega}_0{}^2\beta\Phi_{mk}(\omega_r,X) U_{3k'} \cos m\theta \, dS - \tilde{\Omega}_r{}^2\ddot{a}_k \times$$

$$\int_S \sum_{i=1}^{3} U_{ik'}U_{ik} dS + \epsilon_d a_k \cos\omega t \int_S U_{3k'}(\tilde{L}_{33}U_{3k}) \, dS +$$

$$\epsilon_m \int_C \left( a_k \frac{\partial U_{1k}}{\partial X} U_{1k'} + Z^{**}\tilde{\Omega}_r{}^2 \ddot{a}_k U_{1k} U_{1k'} \right) d\theta \Bigg] = 0 \quad (10)$$

Upon use of Eq. (8), reverting back to the more conventional displacement symbols in Eq. (6) carrying out the spatial integration, this can be written as

$$\sum_{k=1}^{K} [(K_{2k'k} - \epsilon_m K_{4k'k})(\tilde{\Omega}_r{}^2\ddot{a}_k + \tilde{\Omega}_k{}^2 a_k) + K_{3k'k}(\tilde{\Omega}_r{}^2\ddot{a}_k +$$

$$\tilde{\Omega}_k{}^2 a_k)] + \sum_{k=1}^{K} \{a_k\tilde{\Omega}_k{}^2[M_{k'k}(\omega_k) + I_{k'k}] + \ddot{a}_k\tilde{\Omega}_r{}^2[M_{k'k}(\omega_r) +$$

$$I_{k'k}] + a_k N_{k'k} \cos\omega t\} = 0 \quad (11)$$

where $k' = 1,2,3, \ldots, K$, and

$$K_{2k'k} = \int_0^{l/a} U_{mk'}U_{mk} dX \quad (12a)$$

$$K_{3k'k} = \int_0^{l/a} V_{mk'}V_{mk} dX \quad (12b)$$

$$K_{4k'k} = Z^{**} \int_0^{2\pi} U_{lk'}U_{lk} d\theta \quad (12c)$$

$$M_{k'k}(\omega_r) = \beta \frac{\omega_0{}^2}{\omega_r{}^2} \int_0^{l/a} W_{mk'}\Phi_{mk}(\omega_r,X) dX \quad (12d)$$

$$M_{k'k}(\omega_k) = \beta \frac{\omega_0{}^2}{\omega_k{}^2} \int_0^{l/a} W_{mk'}\Phi_{mk}(\omega_k,X) dX \quad (12e)$$

$$I_{k'k} = \int_0^{l/a} W_{mk'}W_{mk} dX \quad (12f)$$

$$N_{k'k} = -\int_0^{l/a} W_{mk'}\left( \hat{N}_{xxd}{}^* \frac{\partial^2 W_{mk}}{\partial X^2} + \frac{\partial \hat{N}_{xxd}}{\partial X}\frac{\partial W_{mk}}{\partial X} - m^2\hat{N}_{\theta\theta d}{}^* W_{mk} \right) dX \quad (12g)$$

The coupled set of $K$ Eq. (11) govern the perturbed motion, described in Fig. 1b, for a given value of $m$. We will limit further discussion to the case of modes having $m \geq 2$. For these modes, the dominant motion is radial for the set of natural modes at lower frequencies. Thus, the terms under the first summation can be neglected, and, in matrix notation, Eq. (11) become

$$\tilde{\Omega}_r{}^2[\tilde{M}]\{\ddot{a}\} + \tilde{\Omega}_k{}^2[\tilde{K}]\{a\} + [\tilde{T}]\{a\} \cos\omega t = 0 \quad (13a)$$

where the elements of the $k'$th row and $k$th column of the corresponding matrices are

$$\tilde{M}_{k'k} = M_{k'k}(\omega_r) + I_{k'k}, \qquad \tilde{K}_{k'k} = M_{k'k}(\omega_k) + I_{k'k}$$

$$\tilde{T}_{k'k} = N_{k'k}; \text{ and } \{a\} = \begin{Bmatrix} a_1 \\ a_2 \\ \cdot \\ \cdot \\ \cdot \\ a_K \end{Bmatrix}$$

Equation (13a) can further be written as

$$\{\ddot{a}\} + (\tilde{\Omega}_k{}^2/\tilde{\Omega}_r{}^2)[\tilde{M}]^{-1}[\tilde{K}]\{a\} + [\tilde{M}]^{-1}[\tilde{T}]\{a\} \cos\omega t = 0 \quad (13b)$$

When the flow is incompressible, $M_{k'k}$ is independent of $\omega$ and we have $[\tilde{M}]^{-1}[\tilde{K}] = [I]$, where $[I]$ is the identity matrix. It must be emphasized that Eqs. (13) are not general differential equations in time but include the restriction of nearly periodic motion in the generalized apparent mass given by Eq. (7).

## Evaluation of Matrix Elements

### Modal Functions

Elements of the matrices in Eqs. (13) will now be evaluated from Eqs. (12d–g) in terms of the $X$-dependent natural modal functions (eigenvectors) of the system. These functions, which are not of closed form, have previously been de-

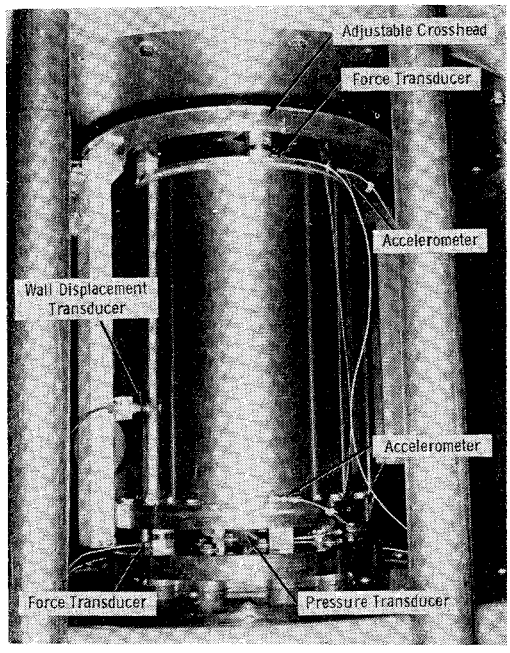


**Fig. 2 Experimental apparatus.**

termined from an eigenvalue problem[4] in terms of the following series forms for the shell displacements:

$$U_{mk}(X) = \tfrac{1}{2}B_{2k}X^2 + B_{1k}(X - l/a) + B_{m0k} + \sum_{n=1}^{N} B_{mnk}\cos\lambda_n X \quad (14a)$$

$$V_{mk}(X) = \sum_{n=1}^{N} C_{mnk}\sin\lambda_n X \quad (14b)$$

$$W_{mk}(X) = \sum_{n=1}^{N} A_{mnk}\sin\lambda_n X \quad (14c)$$

and, for the velocity potential,

$$\Phi_{mk}(\omega_r,X) = \sum_{n=1}^{N} A_{mnk}\Psi_{mn}(\omega_r,X) \quad (15)$$

where $\Psi_{mn}(\omega_r,X)$ is a component function which satisfies Eq. (4) for vibration at frequency $\omega_r$, and corresponds to the $\sin\lambda_n X$ component function in $W_{mk}$ through the boundary condition which must be satisfied at the tank wall.[4]

### Mass Coefficients

The mass coefficient $I_{k'k}$ will now be developed from Eq. (12f). By means of Eq. (14c), there results

$$I_{k'k} = \int_0^{l/a}\sum_{n=1}^{N}\sum_{n'=1}^{N} A_{mnk}A_{mn'k'}\sin\lambda_{n'}X\sin\lambda_n X dX = \frac{l}{2a}\sum_{n=1}^{N}\sum_{n'=1}^{N} A_{mnk}A_{mn'k'}\delta_{n'n} = \frac{l}{2a}\sum_{n=1}^{N} A_{mnk}A_{mnk'} \quad (16)$$

By substituting Eqs. (14c) and (15) into (12d), the liquid apparent mass coefficient corresponding to the response frequency $\omega_r$ becomes

$$M_{k'k}(\omega_r) = \sum_{n=1}^{N}\sum_{n'=1}^{N} A_{mnk}A_{mn'k'}\mathfrak{M}_{n'n}(\omega_r) \quad (17)$$

where

$$\mathfrak{M}_{n'n}(\omega_r) = \beta\frac{\omega_0^2}{\omega_r^2}\int_0^{l/a}\Psi_{mn}(\omega_r,X)\sin\lambda_{n'}X dX$$

Except for a normalizing constant, the latter expression has also been evaluated in previous work. That is,

$$\mathfrak{M}_{n'n}(\omega_r) = \alpha_{n'}{}^2 M_{mn'n} \quad (18)$$

where

$$\alpha_{n'}{}^2 = \int_0^{l/a}\sin^2\lambda_{n'}X dX = \frac{l}{2a}$$

and $M_{mn'n}$ is given by Eq. (18a) in Ref. 4. Note, however, that the free index $k$ used in the referenced expression is not the same $k$ which is used to designate the natural mode herein, and we must also use $\omega_r = \omega$.

Finally, the apparent mass coefficient $M_{k'k}(\omega_k)$ given by Eq. (12e) is obtained simply by substituting $\omega_r = \omega_k$ in Eqs. (17) and (18).

### Parametric Coefficients

Upon substitution of Eq. (14c) into (12g), we obtain

$$N_{k'k} = \sum_{n=1}^{N}\sum_{n'=1}^{N} A_{mnk}A_{mn'k'}J_{n'n} \quad (19a)$$

where

$$J_{n'n} = \int_0^{l/a}\left(\lambda_n{}^2\hat{N}_{xxd}{}^*\sin\lambda_n X - \lambda_n\frac{\partial\hat{N}_{xxd}{}^*}{\partial X}\cos\lambda_n X + m^2\hat{N}_{\theta\theta d}{}^*\sin\lambda_n X\right)\sin\lambda_{n'}X\, dX \quad (19b)$$

The dynamic stress resultant amplitudes $\hat{N}_{xxd}{}^*$ and $\hat{N}_{\theta\theta d}{}^*$ are produced by forced excitation in the axisymmetric initial state described in Fig. 1a. These stress amplitudes can be expressed in terms of the amplitudes of the initial-state displacements by means of the usual stress-displacement equations

$$\hat{N}_{xxd}{}^* = \nu\hat{W}^p + \partial\hat{U}^p/\partial X \quad (20a)$$

$$\hat{N}_{\theta\theta d}{}^* = \hat{W}^p + \nu\partial\hat{U}^p/\partial X \quad (20b)$$

Thus, the parametric coefficients are partly determined by the initial-state displacement amplitudes $\hat{U}^p$ and $\hat{W}^p$.

The solution to the linear forced axisymmetric response of the initial state, in terms of displacements, has previously been given by Eq. (25) in Ref. 4. However, in the direct use of this equation, the appropriate elements of its matrices must include the substitution

$$M^{**} = Z^{**} \text{ for } m = 0, 1 \quad (21)$$

since an arbitrary acceleration impedance is allowed in the present problem, rather than only a rigid mass. Further, to allow for comparison of numerical and experimental data, it is convenient to express the initial-state displacements as ratios of the excitation amplitude $X_0$. Therefore, the dynamic displacement amplitudes are of the form

$$\hat{U}^p = X_0\left[\frac{1}{2}B_2{}^pX^2 + B_1{}^p\left(X - \frac{l}{a}\right) + B_{m0}{}^p + \sum_{n''=1}^{N} B_{mn''}{}^p\cos\lambda_{n''}X\right] \quad (22a)$$

$$\hat{W}^p = X_0\sum_{n''=1}^{N} A_{mn''}{}^p\sin\lambda_{n''}X \quad (22b)$$

whose coefficients are completely determined by solving for the case of $X_0 = 1$.

The initial-state stresses can now be determined. Upon substituting Eqs. (22) and (20a), there results

$$\hat{N}_{xxd}{}^* = X_0\left[B_1{}^p + B_2{}^pX - \sum_{n''=1}^{N}(\lambda_{n''}B_{mn''}{}^p - \nu A_{mn''}{}^p)\sin\lambda_{n''}X\right] \quad (23a)$$

and the derivative is

$$\frac{\partial \hat{N}_{xxd}^*}{\partial X} = X_0 \left[ B_2^p - \lambda_{n''} \sum_{n''=1}^{N} (\lambda_{n''} B_{mn''}^p - \nu A_{mn''}^p) \cos \lambda_{n''} X \right] \quad (23b)$$

Upon substituting Eqs. (22) into (20b), there results

$$\hat{N}_{\theta\theta d}^* = X_0 \left[ \nu(B_1^p + B_2^p X) + \sum_{n''=1}^{N} (A_{mn''}^p - \nu \lambda_{n''} B_{mn''}^p) \sin \lambda_{n''} X \right] \quad (23c)$$

For convenience of computation, these stress resultants and derivatives are expanded into complete Fourier series as follows:

$$\hat{N}_{xxd}^* = X_0 \sum_{n''=1}^{N} N_{1n''} \sin \lambda_{n''} X \quad (24a)$$

$$\hat{N}_{\theta\theta d}^* = X_0 \sum_{n''=1}^{N} N_{2n''} \sin \lambda_{n''} X \quad (24b)$$

$$\frac{\partial \hat{N}_{xxd}^*}{\partial X} = X_0 \left( B_2^p + \sum_{n''=1}^{N} N_{3n''} \cos \lambda_{n''} X \right) \quad (24c)$$

where

$$N_{1n''} = B_2^p \tilde{\chi}_{1n''} + B_1^p \tilde{\chi}_{0n''} - \lambda_{n''} B_{mn''}^p + \nu A_{mn''}^p$$
$$N_{2n''} = A_{mn''}^p + \nu(B_2^p \tilde{\chi}_{1n''} + B_1^p \tilde{\chi}_{0n''} - \lambda_{n''} B_{mn''}^p)$$
$$N_{3n''} = -\lambda_{n''}^2 B_{mn''}^p + \nu \lambda_{n''} A_{mn''}^p$$

and

$$\tilde{\chi}_{0n''} = \frac{2a}{l} \int_0^{l/a} \sin \lambda_{n''} X dX$$

$$\tilde{\chi}_{1n''} = \frac{2a}{l} \int_0^{l/a} X \sin \lambda_{n''} X dX$$

The parametric coefficients can now be complete evaluated. Upon substitution of Eqs. (24) into Eqs. (19), there results

$$N_{k'k} = X_0 \sum_{n=1}^{N} \sum_{n'=1}^{N} A_{mnk} A_{mn'k'} \left[ \sum_{n''=1}^{N} (\lambda_n^2 N_{1n''} d_{n''n'n} + m^2 N_{2n''} d_{n''n'n} - \lambda_n N_{3n''} e_{n''n'n}) - \lambda_n B_2^p e_{0n'n} \right] \quad (25)$$

where

$$e_{0n'n} = \int_0^{l/a} \cos \lambda_n X \sin \lambda_{n'} X dX$$

$$e_{n''n'n} = \int_0^{l/a} \cos \lambda_{n''} X \cos \lambda_n X \sin \lambda_{n'} X dX$$

$$d_{n''n'n} = \int_0^{l/a} \sin \lambda_{n''} X \sin \lambda_{n'} X \sin \lambda_n X dX$$

**One-Term Approximation**

For the $m,k$'th natural mode in Eq. (13a), set $k' = k$ to obtain

$$\tilde{\Omega}_r^2 \bar{M} \ddot{a}_k + \tilde{\Omega}_k^2 \bar{K} a_k + X_0 \bar{T} a_k \cos \omega t = 0 \quad (26)$$

where from Eqs. (16–19)

$$\bar{M} = \frac{l}{2a} \sum_{n=1}^{N} \sum_{n'=1}^{N} A_{mnk} A_{mn'k} M_{mn'n}(\omega_r) + \frac{l}{2a} \sum_{n=1}^{N} A_{mnk}^2$$

$$\bar{K} = \frac{l}{2a} \sum_{n=1}^{N} \sum_{n'=1}^{N} A_{mnk} A_{mn'k} M_{mn'n}(\omega_k) + \frac{l}{2a} \sum_{n=1}^{N} A_{mnk}^2$$

$$\bar{T} = \sum_{n=1}^{N} \sum_{n'=1}^{N} A_{mnk} A_{mn'k} \left[ \sum_{n''=1}^{N} (\lambda_n^2 N_{1n''} d_{n''n'n} + m^2 N_{2n''} d_{n''n'n} - \lambda_n N_{3n''} e_{n''n'n}) - \lambda_n B_2^p e_{0n'n} \right]$$

Equation (26) is a Mathieu equation whose stability properties are well known. To put it in a standard form[8] for determining the stability boundaries for principal parametric ($\frac{1}{2}$-subharmonic) resonance, we set $\omega = 2\omega_r$ and obtain

$$\ddot{a}_k + (\bar{a} + 2\bar{q} X_0 \cos 2\tau) a_k = 0 \quad (27)$$

where $\bar{a} = \tilde{\Omega}_k^2 \bar{K} / (\tilde{\Omega}_r^2 \bar{M})$ and $\bar{q} = \bar{T} / (2\tilde{\Omega}_r^2 \bar{M})$. The stability boundaries can then be approximated by

$$\bar{q} X_0 = \bar{a} - 1 \text{ for } \bar{a} > 1$$
$$\bar{q} X_0 = 1 - \bar{a} \text{ for } \bar{a} < 1 \quad (28)$$

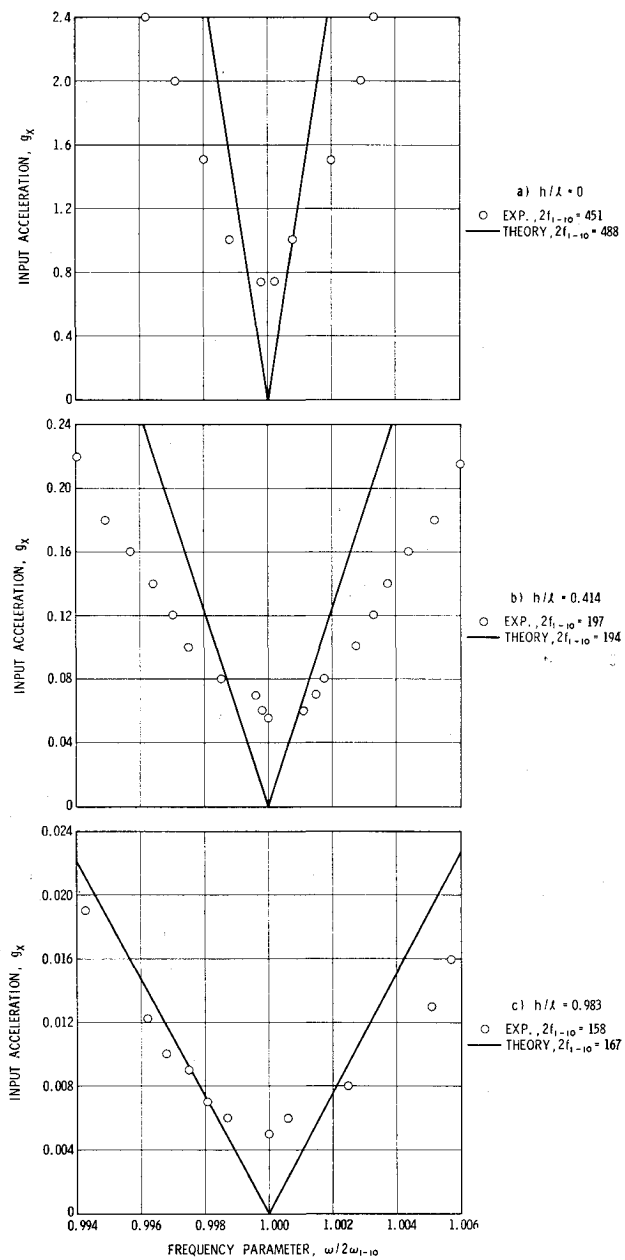


**Fig. 3 Influence of liquid depth on stability; $Z_0$ = 34.53 lb/g, $P_0$ = 34.53 lb, $p_0$ = 0 psig.**

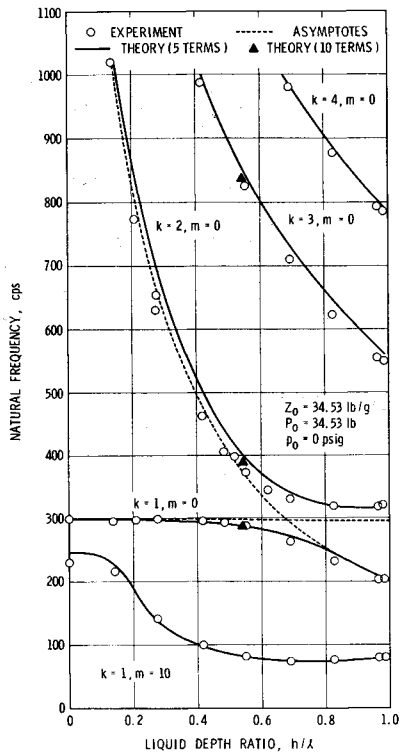


**Fig. 4 Natural frequencies of partially filled tank.**

In terms of input acceleration, which is convenient for experimental measurement, these become

$$g_x = X_0(\omega^2 a/g) = (\omega^2 a/g)(|\bar{a} - 1|/\bar{q}) \qquad (29)$$

## Theoretical and Experimental Results

Experimental data for stability boundaries are obtained from the apparatus shown in Fig. 2. All pertinent parameters, including the input impedance $Z_0$ of the boundary condition at the tank top, could be measured. The use of acceleration impedance (force/acceleration) proved to be most convenient in this application. Variation of the impedance was achieved by using different rigid masses as well as the loading frame. The cylinder is made of 0.005-in. stainless steel, has a diameter of 10 in., and is 14.5 in. long (the same cylinder as that used in Ref. 4).

Theoretical and experimental stability boundaries are compared in Fig. 3 for the $k = 1, m = 10$ mode. Theoretical results are obtained from Eq. (29) with $N = 5$ terms. Excitation conditions at or above the boundaries result in a principal parametric resonance whose mode shape is dominantly the $k = 1, m = 10$ natural mode, and whose frequency of motion is $\frac{1}{2}$-subharmonic to the excitation. Experimental points were determined as the points of least acceleration where the parametric response would occur. It is apparent that sig-

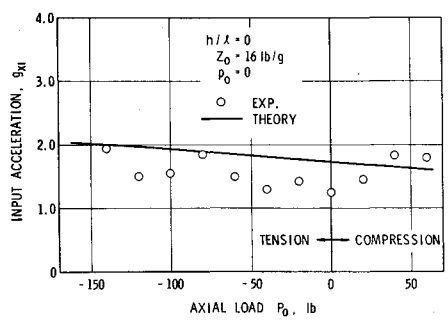


**Fig. 5 Influence of axial load on stability.**

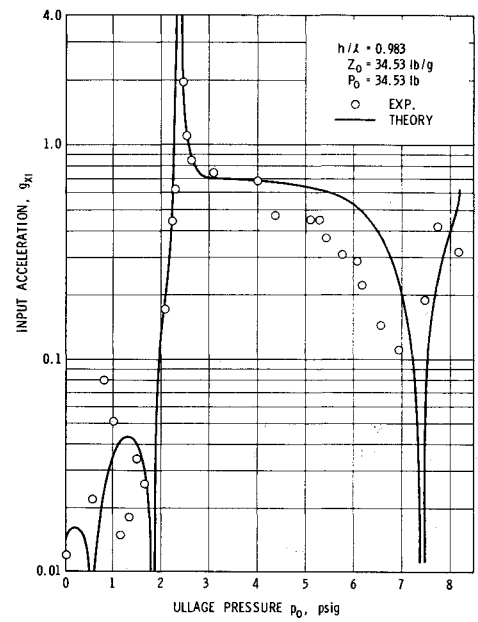


**Fig. 6 Influence of ullage pressure on stability.**

nificant deviation exists between theoretical and experimental results for the empty tank, and better agreement is achieved for greater liquid depths. After careful scrutiny, it was ascertained that the wider experimental stability boundaries are principally caused by imperfections in the cylinder. That is, split natural modes[9] and spatially shifting modal patterns occurred so that one exact natural frequency did not exist. As a result, the experimental system shows a tendency to be more unstable than predicted by theory. This trend is apparent in all the data. It is possible that somewhat better agreement could be achieved by the use of some form of imperfection theory in the analysis. This possibility remains to be investigated.

It was desirable to determine the influence of the various system parameters on the stability boundaries for a given mode. This was done in terms of dimensional variables, in order to emphasize the complexity of this influence. For this purpose, it is necessary to understand the effects of the same parameters on the natural frequencies of the system. For convenience, some natural frequencies which were determined in the earlier work[4] for several symmetric and one nonsymmetric mode are given as functions of liquid depth in Fig. 4.

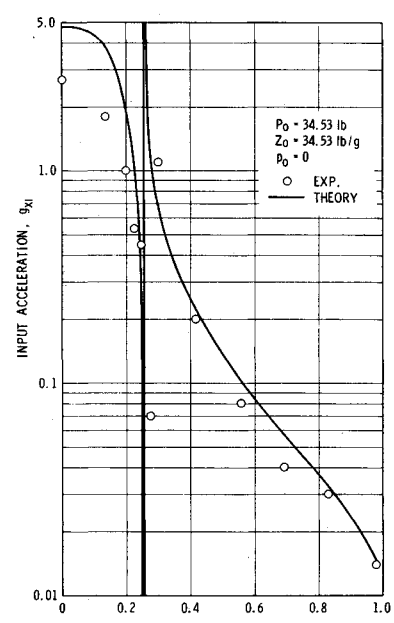


**Fig. 7 Influence of liquid depth on stability.**

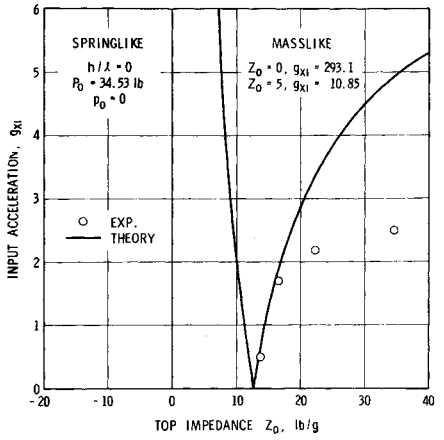


**Fig. 8 Influence of top impedance on stability.**

It is recognized that, in general, a more unstable system will possess a stability boundary whose acceleration ordinate is at a lower value for a given value of the frequency parameter $2\omega_{1-10}$. Therefore, in order to assess the effects of axial load, ullage pressure, liquid depth, and top impedance, a stability boundary acceleration $g_{x1}$ was determined at an excitation frequency value of $\omega_{x1} = 0.996\ (2\omega_{1-10})$ for a range of each of these parameters. Theoretical and experimental results are compared in Figs. 5–8. These results must be compared with those in Fig. 4 for proper interpretation. At a given liquid depth, increasing axial tension has only a small effect on natural frequencies and, likewise, only an insignificant effect on stability as shown in Fig. 5. On the other hand, increasing ullage pressure significantly raises the natural frequencies of the nonsymmetric modes but leaves those of the lower symmetric modes essentially unchanged. Thus, as $\omega_{x1}$ approaches a natural frequency for a symmetric mode, the parametric excitation of the initial state is amplified, and the system becomes more unstable. This is reflected by the dips in the curves in Fig. 6. It is also interesting to note that, at certain frequencies, the system becomes completely stable where the parametric coefficient in Eq. (27) becomes zero.

Increasing liquid depth changes all natural frequencies, as shown in Fig. 4, and has a profound influence on stability throughout the depth range, as shown in Fig. 7. This results from the coincidence of $\omega_{x1}$ with natural frequencies of symmetric modes at certain points, as well as the provision of an increased distributed parametric loading on the tank wall.

The influence of top impedance on stability is shown in Fig. 8. Increasing this impedance lowers the frequencies of symmetric modes while leaving the nonsymmetric mode frequencies unaltered. Thus, strong interaction can again be seen to occur. The dip in the curve occurs at an impedance such that $\omega_{x1}$ coincides with the natural frequency of the first symmetric mode.

It is obvious that variation of the aforementioned parameters can cause either an increase or decrease of stability, depending on the range of analysis. Further, it must be recognized that many nonsymmetric modes are present in the frequency range indicated in Fig. 4, and each mode can become unstable as the one which was studied. Therefore, a complex pattern of instability and parametric resonance occurs with many overlapping regions of instability. The overall trend of the data shows good qualitative agreement between theory and experiment, although significant quantitative discrepancies exist because of the reasons previously discussed.

## References

[1] Bolotin, V. V., *The Dynamic Stability of Elastic Systems*, Holden-Day, San Francisco, Calif., 1964.

[2] Kana, D. D. and Gormley, J. F., "Longitudinal Vibration of a Model Space Vehicle Propellant Tank," *Journal of Spacecraft and Rockets*, Vol. 4, No. 12, Dec. 1967, pp. 1585–1591.

[3] Kana, D. D. and Craig, R. R., Jr., "Parametric Oscillations of a Longitudinally Excited Cylindrical Shell Containing Liquid," *Journal of Spacecraft and Rockets*, Vol. 5, No. 1, Jan. 1968, pp. 13–21.

[4] Kana, D. D. and Chu, W. H., "Influence of a Rigid Top Mass on the Response of a Pressurized Cylinder Containing Liquid," *Journal of Spacecraft and Rockets*, Vol. 6, No. 2, Feb. 1969, pp. 103–110.

[5] Sanders, J. L., Jr., "Nonlinear Theories for Thin Shells," *Quarterly of Applied Mathematics*, Vol. XXI, No. 1, 1963, pp. 21–36.

[6] Sanders, J. L., Jr., "An Improved First Approximation Theory for Thin Shells," Rept. 24, June 1959, NASA.

[7] Duncan, W. J., "Galerkin's Method in Mechanics and Differential Equations," R and M 1798, Aeronautical Research Committee, London, 1937.

[8] Cunningham, W. J., *Introduction to Nonlinear Analysis*, McGraw-Hill, New York, 1958.

[9] Tobias, S. A., "A Theory of Imperfection for the Vibration of Elastic Bodies of Revolution," *Engineering*, Vol. 172, 1951, pp. 409–411.